Narrow Line Structure in the HETG Spectra of NGC 3227

Kendrah D. Murphy[1], Michael A. Nowak[2]

[1]Dept. of Physics, Skidmore College, Saratoga Springs, NY

[2]Dept. of Physics, Washington University, St. Louis, MO

We present an analysis of the Chandra-HETG spectra of the highly variable Seyfert 1.5 galaxy NGC 3227 (z~0.00386), from two observations completed in 2016 and 2017. The first (~30 ks) observation reveals evidence of double-peaked Fe Kα line emission, with centroid energies separated by ~60 eV. The second (~120 ks) observation provides evidence of several emission lines from silicon and sulfur with a range of ionization states that indicate the presence of a warm outflow of material at ~ 600 km/s. Fe XXV and Fe XXVI line features appeared to vary from emission to absorption over the course of the two observations.

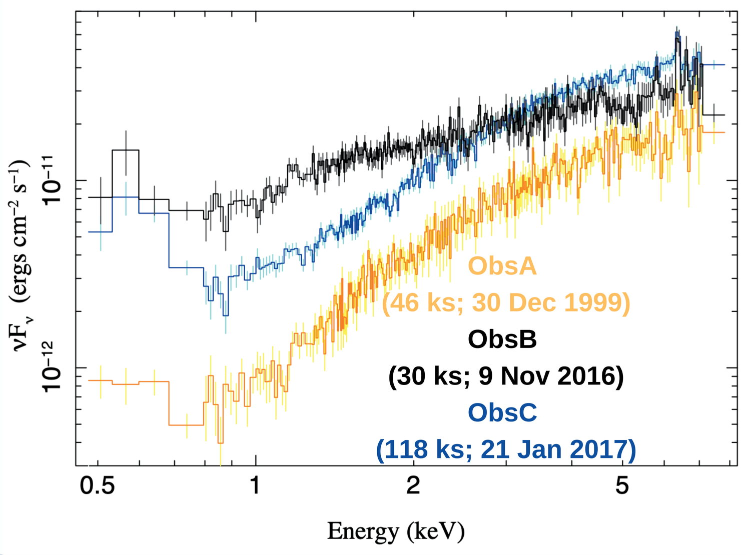

- NGC 3227 was observed three times by the *Chandra* HETGS.
- We used ISIS (Houck et al. 2000) to perform the spectral analysis; plots are shown in the rest frame of NGC 3227.
- ***Left***: The combined 1st order HEG+MEG spectra, with a variable binning for illustration purposes.

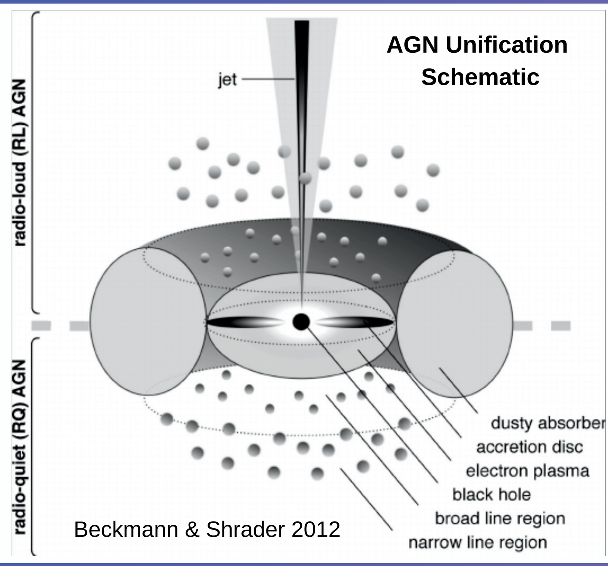

Previous X-ray studies of NGC 3227 have found:

- Fe Kα emission with a FWHM consistent with a BLR origin and line emission at 6.0 keV that may be associated with the red wing of highly-relativistically-broadened Fe K emission or an accretion disk hotspot (*XMM-Newton*; Markowitz et al. 2009).
- Fe XXV and Fe XXVI absorption and variable broad Fe Kα line emission (*Suzaku;* Patrick et al. 2012).
- Strong X-ray variability, with evidence for highly-ionized absorption (e.g., *ASCA*: Ptak et al. 1994, *LETG*: Komossa et al. 2001, and *XMM*: Gondoin et al. 2003).
- An occultation event (~1 day) attributed to a BLR cloud with an outflow velocity ~ 800 km/s (*XMM*; Turner et al. 2018; also see Grafton-Waters et al. 2023). This occured between the ObsB and ObsC HETG observations of NGC 3227.

Fe K Band HEG Fits

Model 1	ObsA	ObsB	ObsB1	ObsB2	ObsC	ObsC1	ObsC2
$I_{\mathrm{FeK}\alpha}$	$1.31^{+108.}_{-0.98}$	$7.12^{+4.11}_{-0.30}$	$6.51^{+6.13}_{-3.43}$	$7.82^{+6.01}_{-5.43}$	$4.33^{+1.84}_{-2.00}$	$4.57^{+3.15}_{-2.51}$	$2.57^{+3.51}_{-1.23}$
$E_{\mathrm{FeK}\alpha}$	$6.387(u)$	$6.427^{+0.019}_{-0.021}$	$6.426^{+0.023}_{-0.032}$	$6.432^{+0.034}_{-0.034}$	$6.399^{+0.019}_{-0.021}$	$6.401^{+0.031}_{-0.034}$	$6.400^{+0.012}_{-0.014}$
$\sigma_{\mathrm{FeK}\alpha}$	$0.005(u)$	$0.040^{+0.020}_{-0.014}$	$0.034^{+0.037}_{-0.020}$	< 0.084	$0.040^{+0.024}_{-0.022}$	$0.047^{+0.039}_{-0.024}$	< 0.037
I_{Fexxv}	$-0.62^{+1.04}_{-0.54}$	$2.00^{+2.11}_{-1.43}$	$1.32^{+3.07}_{-2.59}$	$2.85^{+3.76}_{-2.30}$	$-0.92^{+0.69}_{-0.66}$	$-1.38^{+1.03}_{-0.84}$	$-0.93^{+1.79}_{-0.84}$
E_{Fexxv}	$6.691(u)$	$6.664^{+0.018}_{-0.018}$	$6.662u$	$6.666^{+0.020}_{-0.022}$	$6.697^{+0.014}_{-0.012}$	$6.695^{+0.012}_{-0.012}$	$6.730u$
I_{Fexxvi}	$1.44^{+1.64}_{-1.12}$	$1.62^{+2.28}_{-1.55}$	$1.91^{+4.32}_{-1.91}$	$1.78^{+4.05}_{-2.70}$	$-1.12^{+0.72}_{-0.68}$	$-0.93^{+2.10}_{-1.04}$	$-1.67^{+1.13}_{-0.84}$
E_{Fexxvi}	$6.943^{+0.022}_{-0.021}$	$6.952^{+0.034}_{-0.037}$	$6.941^{+u}_{-0.030}$	$6.961u$	$6.928^{+0.016}_{-0.020}$	$6.933u$	$6.924^{+0.017}_{-0.021}$
C stat/DoF	253.0/203	231.3/203	274.4/203	218.5/203	216.4/203	212.1/203	207.9/203
Model 2							
$I_{\mathrm{FeK}\alpha,a}$	···	$3.05^{+2.53}_{-1.66}$	$3.35^{+3.93}_{-2.12}$	$2.98^{+3.53}_{-2.25}$	$2.21^{+0.99}_{-0.95}$	$1.66^{+1.42}_{-1.19}$	$2.62^{+1.44}_{-1.64}$
$E_{\mathrm{FeK}\alpha,a}$	···	$6.397^{+0.010}_{-0.008}$	$6.402^{+0.012}_{-0.012}$	$6.395^{+0.014}_{-0.015}$	$6.397^{+0.009}_{-0.009}$	$6.391^{+0.020}_{-u}$	$6.350^{+0.057}_{-u}$
$\sigma_{\mathrm{FeK}\alpha,a}$	···	$0.005(f)$	$0.005(f)$	$0.005(f)$	$0.005(f)$	$0.005(f)$	$0.005(f)$
$I_{\mathrm{FeK}\alpha,b}$	···	$3.70^{+2.20}_{-1.77}$	$2.94^{+3.05}_{-2.13}$	$4.08^{+3.84}_{-2.57}$	$-1.04^{+0.91}_{-0.85}$	$-1.75^{+1.49}_{-1.20}$	$-0.19^{+1.70}_{-2.77}$
$E_{\mathrm{FeK}\alpha,b}$	···	$6.458^{+0.015}_{-0.013}$	$6.458^{+0.022}_{-0.024}$	$6.459^{+0.023}_{-0.016}$	$6.446^{+0.021}_{-0.025}$	$6.447u$	$6.400u$
$\sigma_{\mathrm{FeK}\alpha,b}$	···	$0.005(f)$	$0.005(f)$	$0.005(f)$	$0.005(f)$	$0.005(f)$	$0.005(f)$
I_{Fexxv}	···	$1.88^{+2.08}_{-1.43}$	$1.22^{+3.08}_{-2.76}$	$2.71^{+3.78}_{-2.27}$	$-0.97^{+0.68}_{-0.65}$	$-1.48^{+1.05}_{-0.78}$	$-0.81^{+2.56}_{-0.81}$
E_{Fexxv}	···	$6.664^{+0.018}_{-0.017}$	$6.662(u)$	$6.666^{+0.021}_{-0.024}$	$6.697^{+0.012}_{-0.010}$	$6.695^{+0.011}_{-0.011}$	$6.730\ u$
I_{Fexxvi}	···	$1.46^{+2.23}_{-1.84}$	$1.77^{+3.72}_{-1.97}$	$1.62^{+3.93}_{-2.59}$	$-1.18^{+0.71}_{-0.71}$	$-1.05^{+2.05}_{-1.20}$	$1.50^{+0.62}_{-0.61}$
E_{Fexxvi}	···	$6.954^{+0.023}_{-0.040}$	$6.941(u)$	$6.961\ (u)$	$6.927^{+0.013}_{-0.019}$	$6.933u$	$6.924^{+0.016}_{-0.019}$
$I_{6.534\mathrm{keV}}$	···	$-1.73^{+0.90}_{-0.89}$	$-1.87^{+1.21}_{-0.35}$	$-1.65^{+1.61}_{-1.23}$	$0.11^{+0.76}_{-0.68}$	$-0.31^{+1.07}_{-0.87}$	$0.43^{+1.11}_{-0.88}$
C stat/DoF	···	217.7/201	266.3/201	211.9/201	216.1/201	211.5/201	206.0/201

We use Cash statistics and quote errors for the ΔC = 2.71 (90% confidence level for one free parameter).

- We analyzed the unbinned HEG spectra to investigate the presence of narrow line features in the Fe K band.
- A simple power-law model was applied to the 5.5–7.25 keV band.
- Gaussian line components were included to model Fe Kα, Fe Kβ, Fe XXV, and Fe XXVI line feaures.
- The line width and the centroid energy shift of the Fe Kβ emission were tied to those of the Fe Kα emission, and the flux was fixed at 13.5% of the Fe Kα line flux (Palmeri et al. 2003).
- We allowed for Fe xxv and Fe xxvi line emission *or* absorption.
- **Table**: Best-fitting centroid line energies (keV), line widths (keV), and line intensities (10^{-5} γ cm^{-2} s^{-1}) for the full observations (ObsA, ObsB, and ObsC) and for the two halves of each observation (ObsB1, ObsB2, ObsC1, ObsC2).
- **Model 1**: includes a single Gaussian line component to model Fe Kα line emission.
- **Model 2**: includes two Gaussian line components to model Fe Kα (as suggested by the probability histogram **below**).
- Unconstrained centroid line energies within the hard boundaries for Fe Kα (6.3–6.48 keV), Fe Kα,a (6.37–6.42 keV), Fe Kα,b (6.42–6.48 keV), Fe xxv (6.6–6.75 keV), and Fe xxvi (6.9–7 keV) are denoted by (u).
- Fixed parameters are denoted by (f).

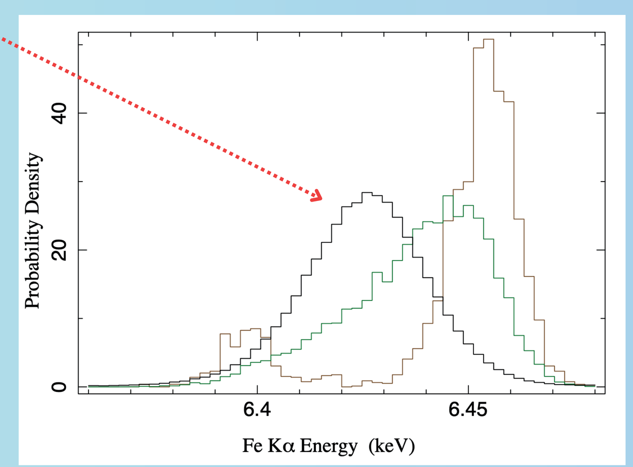

- ***Left***: Probability density histograms showing the posterior likelihood for the Fe Kα rest frame centroid energy value for Model 1 applied to Obs. B.
- The single-peaked histogram (**black**) centered on ~ 6.43 keV is for the full probability distribution. The probability distribution first shifts to higher energy, and then splits into two peaks, as we limit the distribution to line widths σ < 25 eV (**green**) and < 10 eV (**brown**), respectively.

- **ObsB**: Confidence contours show evidence of double-peaked line emission near the rest energy of Fe Kα, with centroid energies at ~6.396 keV and 6.458 keV, respectively.
- The centroid energies of the two lines are different, and both have non-zero equivalent widths, to at least 99% confidence.
- Both halves of the ObsB observation also show evidence of two distinct peaks.

- **ObsC**: Evidence of double-peaked Fe Kα line emission is weaker in the full spectrum, but may be present in the spectrum for the first half of the observation.
- For the full ObsC spectrum (and in the second half of ObsC), single-peaked Fe Kα line emission near 6.4 keV is preferred.

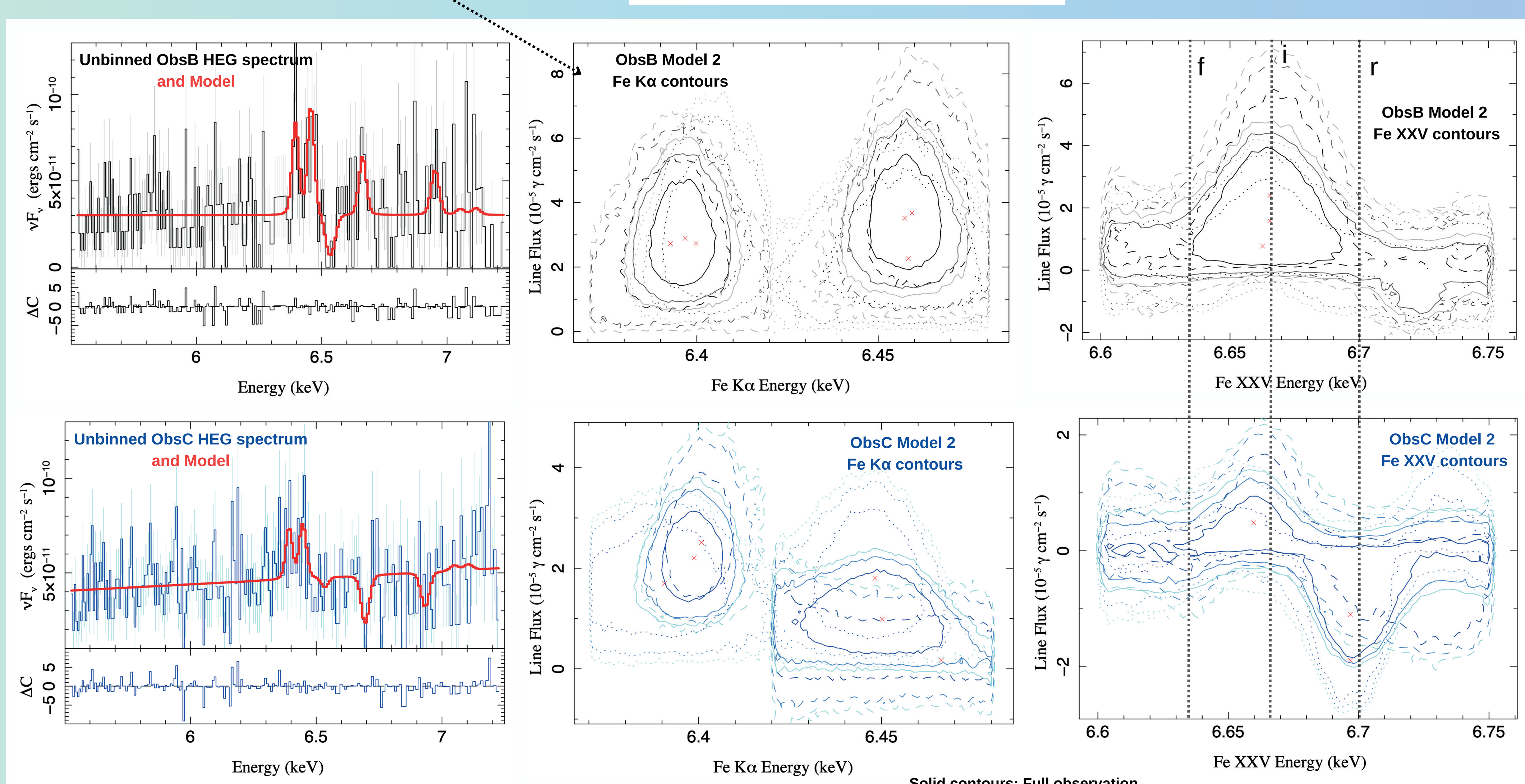

Solid contours: Full observation

Dotted/Dashed Contours: 1st/2nd half of the observation

- Fe XXV emission is favored in ObsB; absorption is favored in ObsC.
- Resonance (r), intercombination (i), and forbidden (f) rest energies are shown with dotted lines.
- Fe XXVI is not well constrained in either of the two observations.

Automated Emission & Absorption Line Search

Identification	Significance # (binned, unbinned)	ΔStatistic (binned, unbinned)	Centroid Rest Energy (keV)	Intensity ($10^{-6}\gamma\,\mathrm{cm}^{-2}\,\mathrm{s}^{-1}$)
Absorption				
Mg XII Lyα	2, 3	−25.7, −21.3	1.473	$-3.546^{+1.113}_{-1.086}$
Si VIII	4, 9	−21.0, −15.9	1.772	$-2.743^{+1.302}_{-1.254}$
Si IX	8, 5	−17.7, −17.6	1.790	$-3.155^{+1.294}_{-1.220}$
Si X	1, 1	−35.1, −35.3	1.808	$-4.127^{+1.052}_{-1.295}$
Si XI	17, N/A	−12.1, N/A	1.828	$-2.184^{+1.550}_{-1.030}$
Si XIII r	3, 2	−34.3, −25.0	1.865	$-4.592^{+1.380}_{-1.318}$
Si XIII Lyβ	24, 24	−11.1, −9.3	2.183	$-3.737^{+2.344}_{-1.131}$
Si XIV Lyα	5, 4	−21.1, −19.4	2.008	$-4.048^{+1.290}_{-1.558}$
S XI	N/A, 11	N/A, −13.8	2.373	$-6.215^{+2.744}_{-2.323}$
S XII	14, 16	−10.6, −11.4	2.395	$-5.515^{+2.284}_{-2.710}$
S XVI Lyα	6, 6	−18.9, −17.0	2.623	$-7.134^{+2.834}_{-2.394}$
Redshift	$-0.0020^{+0.0002}_{-0.0002}$		E = Erest/(1 + z)	
Width Factor	$0.0008^{+0.0002}_{-0.0002}$		σ = E × Width F actor	

- We performed an automated search for narrow emission and absorption lines across the 0.4–9 keV band using the combined HEG+MEG data for ObsB and ObsC, using an algorithm that we developed in ISIS. We then investigated those results through direct fitting of Gaussian line profiles to the spectra. The result is a list of approximate centroid energies for emission and/or absorption lines, in order of their addition to the model, with line #0 being the first added line.
- For the "binned" (S/N≥ 4) spectra, we employed a χ2 fit statistic; for the unbinned data, we applied Cash statistics.

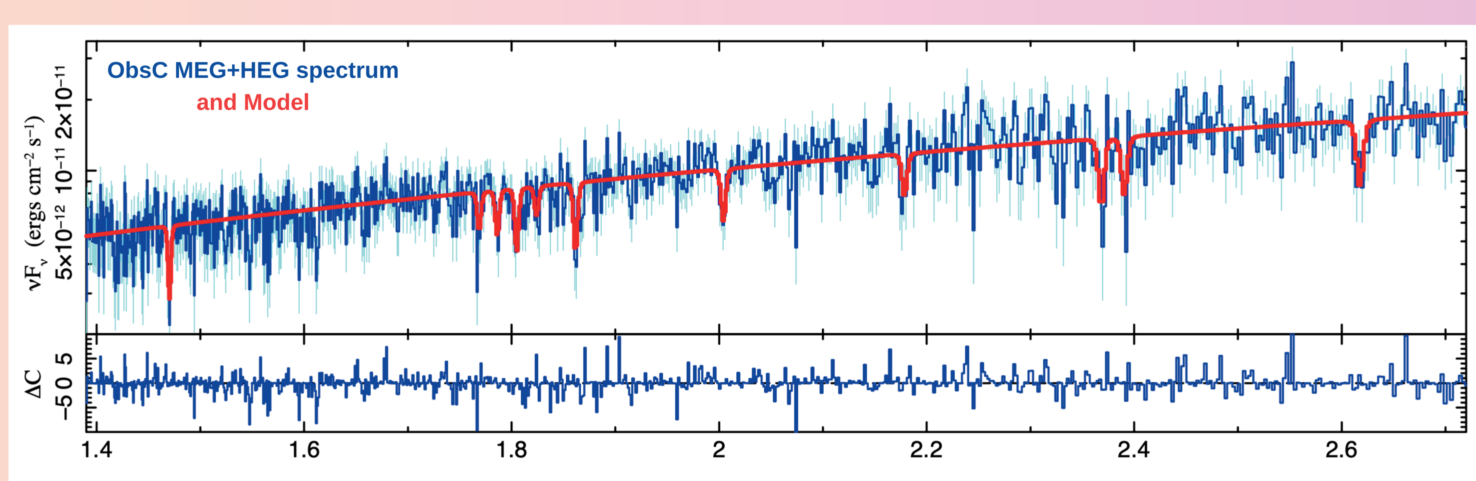

In **ObsC**, 11 absorption lines were found with a common blueshift (z ~ -0.002): Si viii, Si ix, Si x, Si xi, Si xiii r, Si xiii Lyβ, Si xiv Lyα, S xi, S xii, S xvi Lyα, and Mg xii Lyα.

Left: We applied a power law with a high-energy cutoff and a blackbody thermal component as a baseline continuum. Gaussian line components model the 11 absorption lines.

Conclusions

- Line emission near 6.4 keV in ObsB may be characterized by a single Fe Kα emission line with a blueshifted centroid energy (~6.427 keV) and a width σ ~ 40 eV. This width corresponds to a FWHM velocity ~4400 km/s, potentially placing the line-emitting material in the BLR if its motion is Keplerian.
- Alternatively, there may be two narrower lines at ~ 6.397 (possibly associated with the torus) and 6.458 keV (possibly Fe K emission from the accretion disk, or emission from an outflow). Better signal-to-noise data is needed to properly investigate whether this emission may be better described with physical models, e.g., emission from a torus and/or a Kerr disk. Spatially-resolved imaging could reveal whether the emission is extended.
- Our automated line search found 11 absorption lines with the same blueshift in ObsC, including seven different ionic states of Si and three of S, indicating a ~ 600 km/s outflow. The (shorter-exposure) ObsB line-search results are more ambiguous. Those results hint, however, that line emission is more likely in ObsB than in ObsC, consistent with our results for the Fe XXV line feature.

Acknowledgements

Support for this work was provided by NASA through the Smithsonian Astrophysical Observatory (SAO) award number AR8-19015X to KDM and award numberTM1-22003X to MAN.
This work has made use of the AtomDB database and employed data obtained from the Chandra Data Archive provided by the Chandra X-ray Center (CXC).

References

- Ar´evalo, P., & Markowitz, A. 2014, ApJ, 434, 479
- Beckmann, V., & Shrader, C. 2012, "Active Galactic Nuclei"
- Devereux, N., 2021, MNRAS, 500, 786
- Gondoin, P., Orr, A., Lumb, D., et al. 2003, A&A, 397, 883
- Grafton-Waters, S., Mao, J., Mehdipour, M., et al. 2023, A&A, 673, 26
- Houck, J. C., & Denicola, L. A. 2000, in ASP Conf. Ser. 216: Astr. Data Analysis Software and Systems IX, Vol. 9, 591
- Komossa, S., Burwitz, V., Predehl, P., et al. 2001, PASP, 249, 450
- Markowitz, A., Reeves, J. N., George, I. M., et al. 2009, ApJ, 691, 922
- Patrick, A. R., Reeves, J. N., Porquet, D., et al. 2012, MNRAS, 426, 2522
- Ptak, A., Yaqoob, T., Serlemitsos, P. J., et al. 1994, ApJ, 436, 31
- Turner, T. J., Reeves, J. N., Braito, V., et al. 2018, MNRAS, 481, 2470